Title

Bioinspired Metal-Ligand Networks with Enhanced Stability and Performance: Facile Preparation of Hydroxypyridinone (HOPO)-Functionalized Materials.

Journal

Macromolecules, 57(24)

ISSN

0024-9297

Authors

Shannon, Declan

Cerdan, Kenneth

Kim, Minseong

et al.

Publication Date

2024-12-24

DOI

10.1021/acs.macromol.4c02250

Peer reviewed

Macromolecules

pubs.acs.org/Macromolecules
Article

Bioinspired Metal–Ligand Networks with Enhanced Stability and Performance: Facile Preparation of Hydroxypyridinone (HOPO)-Functionalized Materials

Declan P. Shannon, Kenneth Cerdan, Minseong Kim, Matthew Mecklenburg, Judy Su, Yueyun Chen, Matthew E. Helgeson,* Megan T. Valentine,* and Craig J. Hawker*

Cite This: *Macromolecules* 2024, 57, 11339–11349

Read Online

ACCESS | Metrics & More | Article Recommendations | Supporting Information

ABSTRACT: Bioinspired hydroxypyridinone (HOPO)-functionalized materials are shown to display a remarkable capacity for stability and for chelating a wide array of metal ions. This allows for the synthesis of multifunctional networks with diverse physical properties when compared to traditional catechol systems. In the present study, we report a facile, one-pot synthesis of an amino HOPO ligand and simple, scalable incorporation into PEG-acrylate based networks via active ester chemistry. This modular network approach allows for fabrication of patterned HOPO containing networks which can chelate a range of metal ions, such as transition metals (Fe^{3+}) and lanthanides (Ho^{3+}, Tb^{3+}), leading to modulation of mechanical, magnetic, and fluorescent properties. Moreover, networks with tailored, heterogeneous properties can be prepared through localization of metal ion incorporation in 3-dimensions via masking techniques, creating distinctly soft, hard, magnetic, and fluorescent domains.

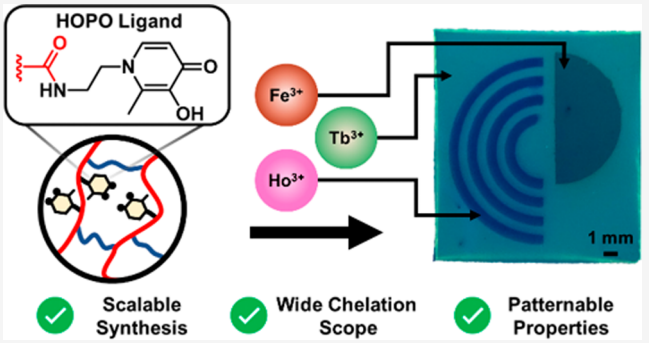

INTRODUCTION

Biomimetic and bioinspired polymer network systems display a wide range of remarkable properties with tailored mechanical responses,[1−3] chemical diversity,[4] and stimuli responsive behavior.[5] Synthetic design of such materials has borrowed, mimicked, and expanded upon natural motifs and represents an enticing area of research with a variety of synthetic strategies available for network formation and property modulation.[1−3,5] While traditional approaches based on building blocks such as catechol derivatives have demonstrated success in preparing bioinspired materials with controlled mechanical responses,[6−10] there is a great interest in developing stable, biomimetic materials with added functionalities and stimuli responsive characteristics for applications ranging from membranes and sensors to soft robotics and magnetic tweezers.[5,11−15] Particularly desirable in these latter domains are capabilities such as lanthanide chelation to impart luminescent and magnetic properties, as they offer rapid responses with facile control of external stimuli.[16] While strategies exist to target such behaviors, implementing user-friendly modular designs at the molecular level is challenging and can often require repeated design of chemical motifs for property modulation.[5]

In pursuit of functional, resilient network materials, various building blocks have been employed to create materials with desirable properties. A wide array of bioinspired approaches exist, with examples ranging from embedded (nano)particulate fillers[12,16,17] to controlling physical properties via metal–ligand chelation.[3,18−22] In particular, use of metal–ligand bonding has been a cornerstone of widely studied metallo-supramolecular networks, which have achieved a wide array of desirable properties, including but not limited to modulation of mechanical, magnetic, luminescent, and self-healing properties.[23−27] While fundamental work from such coordination polymer literature has provided a basis for metal–chelating polymer networks, the present research focuses on building these foundational motifs into dual-network materials composed of both covalent and metal–ligand bonds. Covalent polymer networks and modulation of their properties play critical roles in a range of systems, including hydrogels, membranes, and even soft robotics. Through decoration of metal–ligand cross-linking sites within the network, properties of the parent, covalent networks can therefore be further tuned via the selection of both ligand and metal ion, providing a facile

Received: September 17, 2024
Revised: November 19, 2024
Accepted: November 22, 2024
Published: December 6, 2024

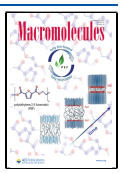

https://doi.org/10.1021/acs.macromol.4c02250
Macromolecules 2024, 57, 11339–11349

Scheme 1. Synthesis of Amine-Terminated HOPO Ligand

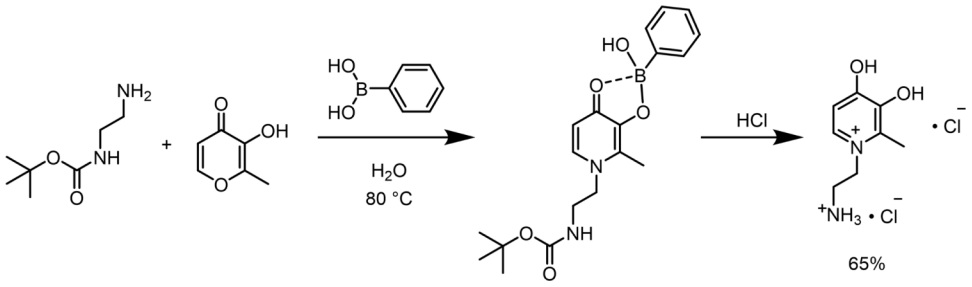

route to metal chelating networks amenable to applications in systems such as sensors, and membranes for lanthanide separation.[3,28−31] Moreover, the metal-ion chelation enables diverse properties to be tuned within the same bioinspired polymer network scaffold as a function of the metal ion used, and for these properties to be selectively localized via soft lithography techniques.[19,21] In particular, the ability to chelate mixtures of transition metal and lanthanide ions is of interest for their ability to form mechanically robust cross-linking sites, as well as for their unique magnetic and optical properties.[3,19,32] As such, there is a present interest in developing methods for preparing functionalized polymer network scaffolds capable of these functions.

Covalent polymer networks incorporating metal−ligand building blocks often take inspiration from the chemical structures of well-studied natural systems which utilize transition metal coordination,[3] including marine mussels,[33] invertebrate jaws,[34−37] tunicates,[38] and others,[39−41] with more recent developments highlighting lanthanide-based systems in bacteria.[42−44] While bioinspired motifs such as catechols have been widely studied, mimosine-mimetic functionalities containing the hydroxypyridinone (HOPO) motif have emerged as a useful class of chelating ligands[45−48] based on their function in mimosoid plants for ion transport.[49,50] These mimosoid plant inspired ligands offer structural similarities and a range of attractive features analogous to siderophore-mimetic catechol ligands, but with increased stability,[51] resistance to oxidation, and wider scope for the chelation of both transition metals and rare earth elements.[45,48,52−55] As such, plant inspired, HOPO-containing small molecules have been employed in metal chelating drugs such as deferiprone and as ligand scaffolds for medical and imaging applications.[45,56−58] Despite their small molecule utility, the preparation of polymeric networks based on HOPO is understudied in the literature,[51,55,59] likely owing to challenges with the multistep synthesis of functional HOPO building blocks.[45] As such, there is a need for straightforward network functionalization strategies to expand the use of the HOPO motif in comparison to other siderophore analogues and to enable potential screenings in synthetic membranes and magnetic soft material applications.

In the present study, we demonstrate a user-friendly and scalable synthetic method for the preparation of HOPO functionalized networks through postpolymerization modification of active ester networks. The potential of these systems is two-fold. We demonstrate facile and scalable installation of HOPO motifs into networks via postpolymerization modification, allowing for comparison to other metal chelating ligands without concerns of changing network topology or monomer reactivity ratios. Secondarily, we demonstrate the utility of the HOPO ligand as a versatile motif for tuning an array of material properties by expanding beyond classical iron chelation examples to tune network mechanical, magnetic, and fluorescent properties through the patterned incorporation of multiple metal ions, both individually and as mixtures. Using recently developed boronic acid chemistry,[60] an amino-functionalized HOPO ligand compatible with active ester chemistry and PEG-acrylate cross-linked networks is reported and directly compared to the corresponding catechol functionalized derivatives.[21,29] This versatile and efficient strategy allows parent covalent networks to be functionalized with HOPO building blocks and the chelation of transition metals such as iron studied for mechanical reinforcement[55] and/or lanthanides examined for the preparation of samples with inherent paramagnetism and UV-induced fluorescence through holmium and terbium cations.[32,45,52,61,62] Building upon prior patterning methods based on selective solution exposure,[19,21] the ability to spatially control metal center incorporation is demonstrated for the preparation of heterogeneous, composite-like materials with localized mechanical, magnetic, and fluorescent behaviors based on multiple metal ion chelation.

RESULTS AND DISCUSSION

A recent hydroxypyridinone (HOPO) synthesis was employed to prepare an active ester compatible HOPO ligand on a multigram scale in a one pot approach. Classic preparation methods[45,55,59] for HOPO derivatives require hazardous reagents and crucially require a multistep synthesis process with multiple protection/deprotection reactions for the starting maltol. To circumvent these limitations, we leveraged the method developed by Ke and coworkers[60] to prepare amino-functionalized HOPO from simple starting materials using water as the solvent (Scheme 1). This facile approach allows for multigram scale preparation from cheap reagents, which further enables large scale preparation of HOPO functionalized networks. In brief, maltol was reacted with *N*-boc-ethylene diamine in the presence of phenylboronic acid to create the protected hydroxypyridinone intermediate. The product as a viscous oil was deprotected in situ with concentrated hydrochloric acid and purified via recrystallization.[63] Detailed synthetic methods and characterizations for the HOPO ligand are included in the Supporting Information.

PEG-acrylate network chemistries were selected as a representative network composition due to their wide adoption in hydrogels, membranes, and soft robotic systems,[15,29] and functionalized networks were then prepared from a solvent free PEG-acrylate monomer mixture. Resin compositions contained pentafluorophenyl acrylate (PFPA, active ester), PEG-diacrylate (PEGDA, M_n = 700 g/mol, cross-linker), PEG-acrylate (PEGMEA, M_n = 480 g/mol, diluent monomer), and a small amount of 2,2-dimethoxy-2-phenylacetophenone

https://doi.org/10.1021/acs.macromol.4c02250
Macromolecules 2024, 57, 11339−11349

Scheme 2. (Top) Installation of HOPO Ligand into PFPA Networks and (Bottom) Complexation with Metal Salts in Aqueous Media[a]

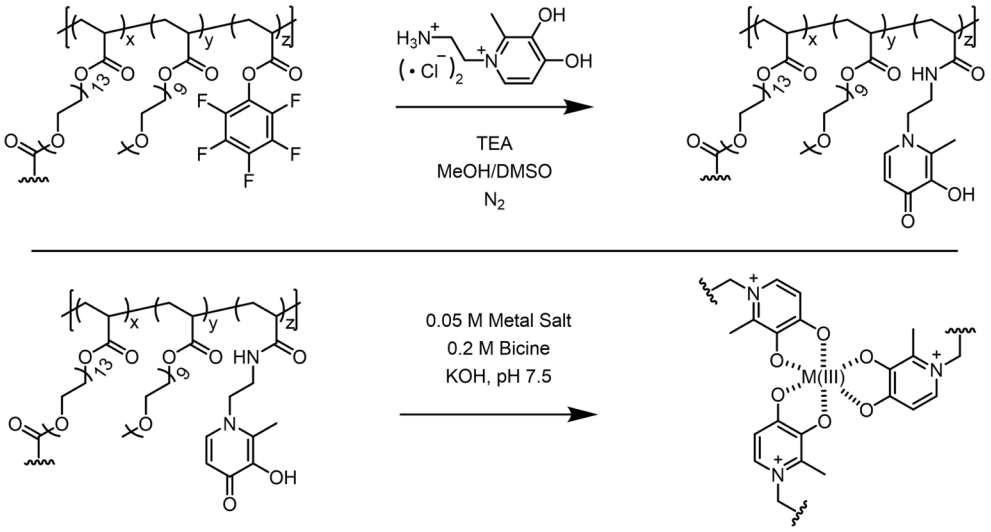

[a]Complexation was conducted with $Fe(NO_3)_3$, $Ho(NO_3)_3$, and $TbCl_3$.

(DMPA, 0.1 wt.%) as a photoinitiator.[21,29] This resin mixture was dispensed between quartz plates with the film thickness controlled by spacer gauges followed by an UV-curing for 2 min (365 nm, 3 mW/cm^2) to form free-standing cross-linked films. Demonstration film compositions utilized a mixture of 3/39/58 mol % PEGDA/PEGMEA/PFPA, with high PFPA content selected for consequentially high ligand content, leading to improved resolution in metal center patterning demonstrations (vide infra), and film compositions for comparison to prior work on catechol functionalized materials.[21]

To compare and contrast the properties of the final HOPO functionalized networks with traditional catechol systems, parent PFPA networks were then substituted with either the synthesized amino-functionalized HOPO derivative (Scheme 2 and Supporting Information) or commercially available dopamine (2-(3,4-dihydroxyphenyl)ethylamine hydrochloride salt) following reported procedures.[21] A major advantage of this building block approach for network functionalization is the ability to obtain films with the same cross-link density and functionalization level to facilitate comparisons between different functional chemistries, without concerns of major topological changes due to changes in network preparation conditions.[21,29,64] Moreover, for both catechol- and HOPO-functionalized networks, metal ions could be incorporated using the same procedures as described previously,[20,21,65] specifically bicine buffered solutions at pH 7.5. Iron was initially selected for mechanical reinforcement of HOPO networks[55] with lanthanide ions being selected based on their magnetic (Ho^{3+} and Tb^{3+}) and fluorescent (Tb^{3+}) properties. It should be noted that the inclusion of Ho^{3+} and Tb^{3+} ions also results in mechanical reinforcement (vide infra). Following metal center installation, but samples were thoroughly dialyzed for 3 days with daily exchange in deionized water to remove residual salts and buffer components and then deswollen using a series of solvent gradients with decreasing polarity.

Effective preparation of active ester networks and quantitative incorporation of the respective ligands into the PEG-acrylate network was validated via FTIR spectroscopy which confirmed full substitution of pentafluorophenyl active ester groups.[21,29] Figure 1 demonstrates the presence of key

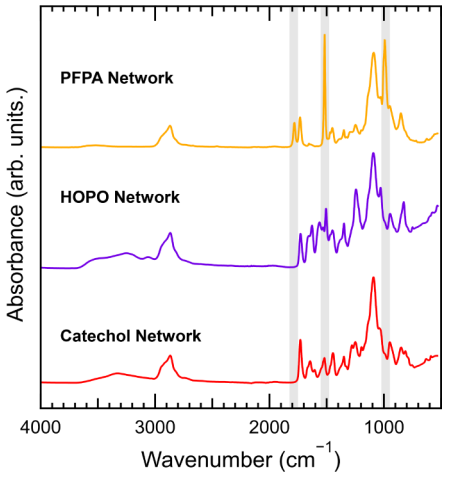

Figure 1. FTIR–attenuated total reflection (ATR) of the random copolymer networks. From top to bottom: a 3/39/58 mol % PEGDA/PEGMEA/PFPA network before substitution (yellow), a PEG-acrylate network after substitution with hydroxypyridinone ligand (purple), a PEG-acrylate network after substitution with dopamine (red). Diagnostic peaks from the PFPA moieties (gray highlighted peaks) at 985, 1520, and 1780 cm^{-1} disappear after reaction with amine ligands with amide stretching bands appearing at ~1660 cm^{-1}.

diagnostic peaks from the pentafluorophenyl group at 985, 1520, and 1780 cm^{-1} in the precursor networks and the disappearance of these peaks upon substitution with an amine terminated ligand. For both catechol- and HOPO-functionalized networks, an amide stretching band at ~1660 cm^{-1} is observed after amidation.

To further confirm the quantitative nature of the substitution reaction, a soluble, linear polymer analogue was prepared and used for diagnostic NMR spectroscopy studies to highlight the facile incorporation of the HOPO unit. In this case, a linear precursor was prepared by free radical

https://doi.org/10.1021/acs.macromol.4c02250
Macromolecules 2024, 57, 11339–11349

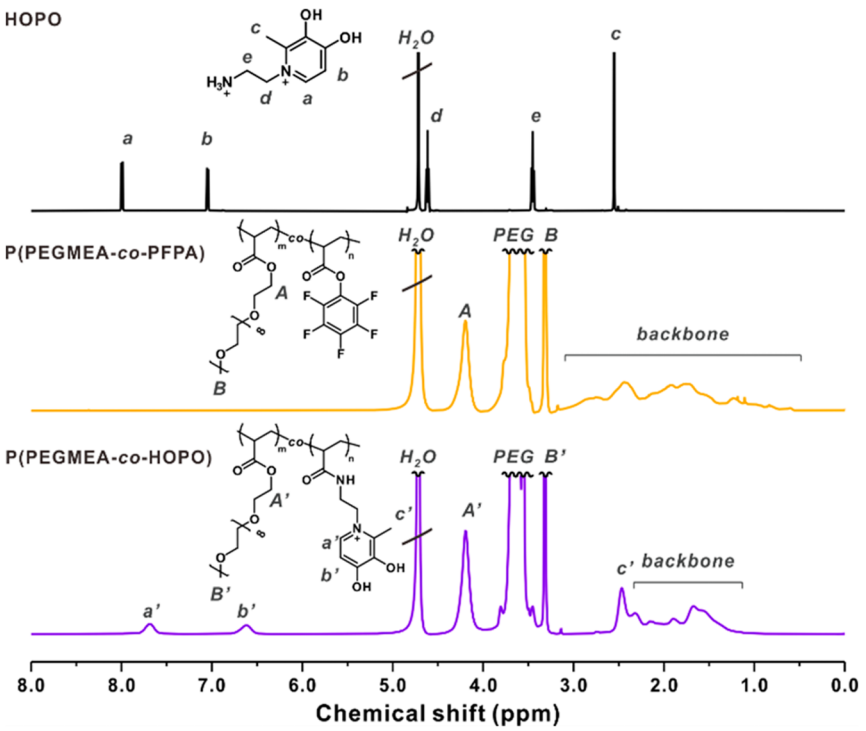

Figure 2. Top to bottom, ^{1}H NMR spectra of the free HOPO ligand, starting PFPA-*co*-PEGMEA linear active ester copolymer, and the substituted HOPO-functionalized copolymer. Key aromatic resonances (a′ and b′) are noted upon substitution of PFPA sites with HOPO functionalities, and additional spectra (^{13}C, ^{19}F, integrated ^{1}H, etc.) are included in the Supporting Information.

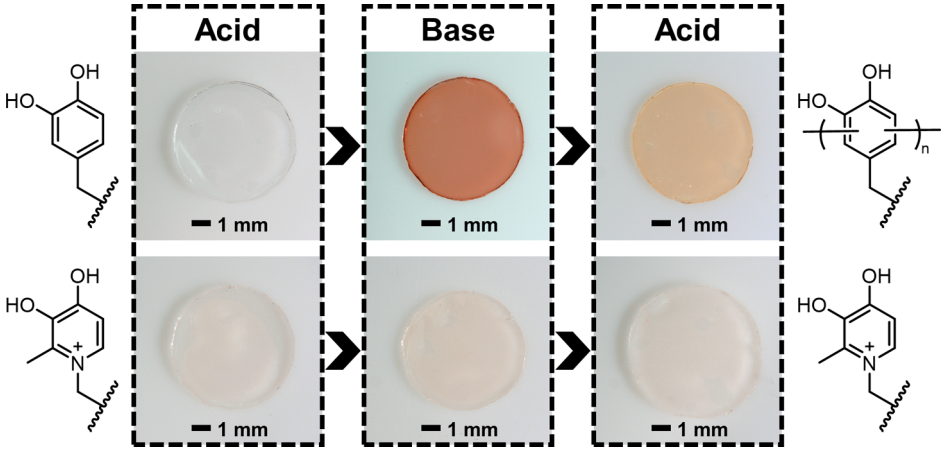

Figure 3. A visual comparison of the oxidative stability for catechol (top row) and HOPO (bottom row) functionalized networks. From left to right, samples before, during, and after 24 h of aging in basic, aqueous media under normal atmospheric conditions. Samples stored in 1 mM HCl solutions were transferred to KOH solutions buffered with bicine (0.2 M) at pH 9 for 24 h followed by dialysis and equilibration in 1 mM HCl storage solution.

copolymerization of PFPA and PEGMEA, followed by substitution with the amine terminated HOPO ligand using a procedure comparable to that developed for network substitution (Supporting Information). As seen in Figure 2, active ester motifs are efficiently substituted with the amine terminated ligand, producing unique diagnostic resonances in the aromatic region, as well as changes in the backbone resonances upon acrylamide formation.[63,66] It was also noted that the pendant HOPO resonances in the aromatic region were observed to shift with the relative pH of the solution and protonation of the ring as noted previously by Gomes et al.[63] Further characterization of substituted materials by NMR spectroscopy (^{13}C, ^{19}F, etc.) is included in the Supporting Information.

To highlight the stability of HOPO-functionalized networks prior to chelation relative to their traditional catechol counterparts, a set of pH mediated aging experiments were conducted. Catechol-containing materials demonstrate limited stability, particularly under basic oxygenated conditions, with known pH-dependent oxidation and autoxidation leading to coloration and cross-linking between neighboring catechol moieties.[10,67,68] Conversely, HOPO containing materials demonstrate significantly improved stability under the same conditions, in part due to changes in electron density in the heteroaromatic ring.[45,51,55,59] As visually demonstrated in

https://doi.org/10.1021/acs.macromol.4c02250
Macromolecules 2024, 57, 11339−11349

Figure 3, disk samples of HOPO and catechol functionalized networks were transferred from acidic storage solutions (1 mM HCl) to basic, aqueous solutions buffered at pH 9 (KOH and 0.2 M bicine) for 24 h, imaged, and then returned to acidic solution. Catechol samples displayed characteristic color changes related to quinone formation and oxidative coupling,[10,51,67] while no appreciable changes were observed for HOPO-functionalized materials, consistent with prior studies.[51,55] This difference in visual appearance between catechol and HOPO systems after base mediated oxidation was further illustrated by FTIR measurements at 24 and 72 h, and via comparison with the FTIR spectra of control, pristine samples and via comparison to controls oxidized with sodium periodate ($NaIO_4$) (Figure S5). For the catechol samples, peaks due to quinone formation were apparent,[69−71] while negligible changes in the FTIR spectra were observed for HOPO samples. Further characterization of base treated HOPO and catechol films was conducted via UV−vis measurement (Supporting Information). Results demonstrated appreciable changes in spectra morphology for base treated catechol samples, while only minimal changes were observed for HOPO networks. Present observations are in line with expectations and prior stability characterization by Andersen et al.[51] These results highlight the stability of the HOPO motif under these conditions compared to traditional siderophore mimetic catechol moieties.

To build desired material properties into these modular networks, an array of metal ions was selected to complex with mimosine-inspired HOPO ligands to tailor mechanical, magnetic, and fluorescent properties. Additionally, to demonstrate potential applications of the HOPO system, strategies were developed for spatially patterned metal chelation to localize mechanical, magnetic, and fluorescent responses using methods previously delineated in the literature.[19,21,61−64] To illustrate the incorporation of different metal cations, a 3/39/58 mol % PEGDA/PEGMEA/PFPA network was prepared as a standard parent film with the functionalized networks being characterized after metal center installation via a combination of Raman spectroscopy and scanning electron microscopy (SEM). Prior literature[21,33] has demonstrated the utility of Raman spectroscopy for confirming the presence of metal−ligand chelation in polymer networks, and comparable approaches were used in this study to elucidate the nature of HOPO−metal center cross-links. Crucially, as seen in Figure 4, diagnostic peaks are observed for the HOPO units in the metal-free parent sample (686 cm^{-1}) which change dramatically after iron chelation (~570 cm^{-1}), in agreement with literature reports for iron−hydroxypyridinone complexes, confirming the introduction of Fe^{3+}−HOPO cross-links.[72] Similarly, Raman spectroscopy provides support for the formation of HOPO−lanthanide complexes. While literature reports of Raman spectra for this metal−ligand complex are sparse, comparable vibrational spectroscopy studies have been conducted with tropolone−lanthanide and tropolone−transition metal complexes which demonstrate similar diagnostic peak shifts from the metal-free to metal-complexed systems.[73−75] A diagnostic peak shift from the metal-free ligand (686 cm^{-1}) to the metal-complexed sample (approximately 705 cm^{-1}) is observed and attributed to changes in ring and M−O vibrational modes upon chelation as seen in the Ho^{3+}−HOPO sample (Figure 4 and Supporting Information for additional metal salts).

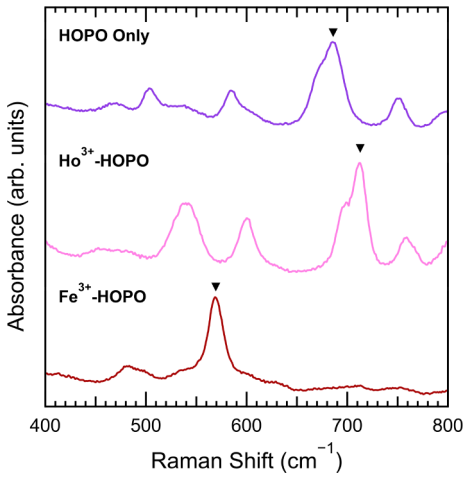

Figure 4. Raman spectra of HOPO-functionalized networks with and without metal ions. From top to bottom: a 3/39/58 mol % PEGDA/PEGMEA/PFPA network after HOPO substitution (purple), a HOPO containing network of the same composition after complexation with Ho^{3+} (pink), and a HOPO network of equivalent composition after complexation with Fe^{3+} (red).

The impact of a tunable metal−ligand-based network on the parent PEGDA covalent network was studied by comparing the mechanical and magnetic properties of bulk, homogeneous and patterned HOPO-functionalized networks with both the parent network as well as the corresponding catechol-functionalized systems. Mechanical behavior of homogeneous polymer networks was initially examined in a three-point bend test with the results demonstrating a significant increase in elastic modulus after metal center incorporation (Figure 5a). For Fe^{3+}-based materials, catecholate and HOPO-functionalized materials both demonstrate high elastic moduli after complexation, relative to their metal-free networks, indicating formation of elastically active metal−ligand cross-links compared to their metal-free base networks (elastic moduli of 3.1 MPa for metal-free catechol networks and 3.8 MPa for metal-free HOPO samples). While some oxidation is anticipated in the Fe^{3+}−catechol system, prior work has shown that the metal−ligand cross-linking and microstructure account for the bulk of the mechanical reinforcement,[20,21,65] and iron ions in solution can serve a protecting role in reducing the rate of oxidative catechol−catechol coupling at mildly basic pH.[67] However, the advantages of the HOPO ligand relative to traditional catechol systems are readily observed following complexation with lanthanide ions. Appreciable differences in elastic moduli were noted, with HOPO networks demonstrating high elastic moduli when complexed with Ho^{3+} (~300 MPa) while catechol-functionalized materials increased to only moderate elastic moduli after Ho^{3+} incorporation (~12 MPa). At present, these mechanical changes for catechol−lanthanide samples are predominantly attributed to oxidation of catechol residues,[21,33] and some potentially weak or unstable capture of lanthanide ions by catechol moieties, but at insufficient levels to provide significant mechanical reinforcement, in line with prior observations by the Raymond group.[76] Moreover, while diagnostic catechol−lanthanide peaks could not be identified via Raman spectroscopy, a paramagnetic moment was observed in magnetometry (vide infra) indicating the presence of trace paramagnetic Ho^{3+} ions in agreement with minor amounts of holmium being detected by scanning electron microscopy−energy dispersive X-ray spectroscopy (SEM−

https://doi.org/10.1021/acs.macromol.4c02250
Macromolecules 2024, 57, 11339−11349

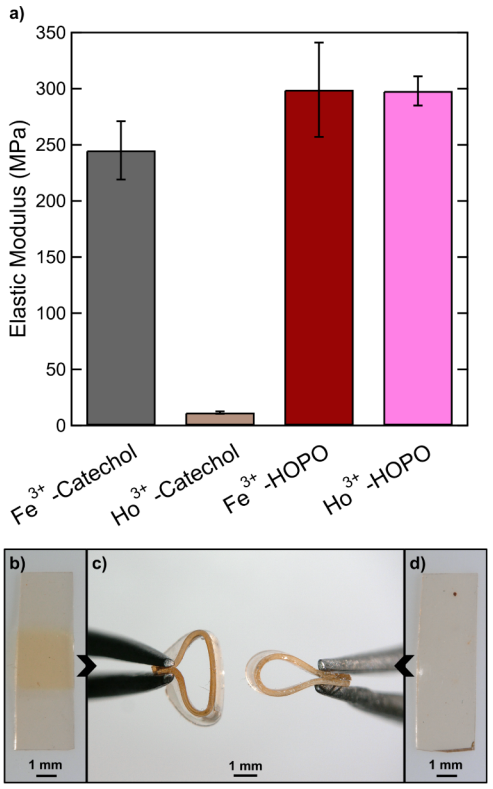

Figure 5. (a) Elastic moduli, *E*, measured via 3-point beam bending of dry, homogeneous, metal−ligand polymer networks. Error bars represent standard deviations from the replicate measurements. Iron−catechol elastic moduli and standard deviation were taken from previous publication using the same preparation and network composition.[21] (b) Polymer film of a 3/39/58 mol % PEGDA/PEGMEA/HOPO network functionalized with Ho^{3+} cations only in the middle, pale, yellow-colored square. (c) Comparison of film mechanical behavior under bending between Ho^{3+}-patterned (left) and metal-free systems (right), demonstrating the heterogeneous mechanical response of the patterned sample. (d) Parent polymer film of 3/39/58 mol % PEGDA/PEGMEA/HOPO without any metal ions installed in the network showing homogeneity of the bulk system.

EDS). Figure 5a clearly illustrates the differences in mechanical reinforcement achieved through secondary catechol and HOPO networks after chelation with either iron or holmium complexes (for additional mechanical testing data and methodology, see the Supporting Information). These mechanical differences show the ability of HOPO ligands to chelate a wide variety of metal ions while also highlighting the limitation of catechol systems for lanthanide capture from aqueous media in mildly basic pH.[45,76]

As a further demonstration of both mechanical reinforcement and the ability to pattern networks via HOPO-functionalized materials, a parent bulk HOPO network was patterned by only exposing the central portion of the film to Ho^{3+} cations. In a classical bending demonstration, the metal-complexed region of the film (Figure 5b,c, center pale yellow region) displays significantly increased rigidity and resistance to bending in comparison to both the regions not exposed to Ho^{3+} as well as a metal-free HOPO control sample (Figure 5c,d), resulting in deformation for the patterned sample only in the metal-free regions. These results highlight the versatility of HOPO-functionalized PEGDA covalent networks for preparing mechanically heterogeneous composite-like materials with tailored properties using a second metal−ligand network based on transition metals as well as lanthanide cations.

To further illustrate the potential properties of the HOPO networks, magnetometry measurements were conducted to probe the strong paramagnetic response of the lanthanide−HOPO networks. Data for homogeneous catechol and HOPO-functionalized films after complexation with holmium are presented in Figure 6a and reveals clear differences in the

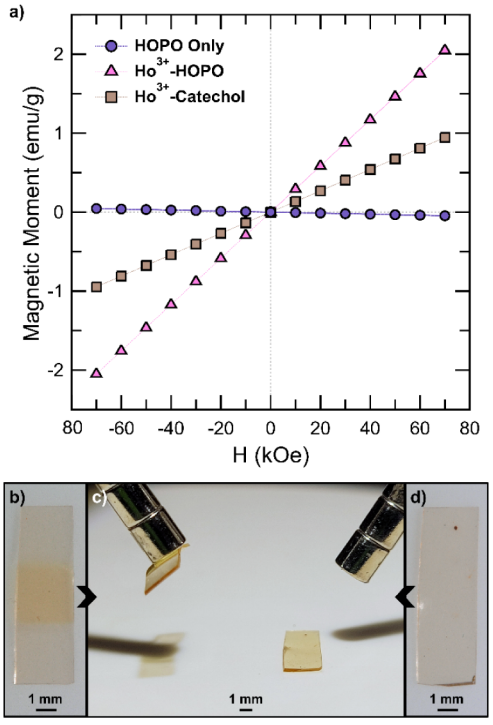

Figure 6. (a) Magnetization curves of bulk, homogeneous holmium Ho^{3+} complexed polymer networks substituted with either catechol (light brown squares) or HOPO (pink triangles) moieties. A metal-free HOPO network (purple circles) is provided for comparison. (b) Polymer film of 3/39/58 mol % PEGDA/PEGMEA/HOPO with a central section functionalized with Ho^{3+}−HOPO complexes via surface patterning. (c) Still image showing the HOPO−Ho^{3+} patterned film being lifted by a magnet in contrast to the metal-free control film. Video format is viewable online in Movie S1. (d) Polymer film of 3/39/58 mol % PEGDA/PEGMEA/HOPO with no metal ion coordination.

magnetic response of each respective film. While both systems display a paramagnetic response, HOPO films show a significant increase in magnetic moment per gram of material for the same applied field compared to that of the catechol-functionalized system. While chelation of lanthanides by catechol-functionalized networks was not observed via Raman spectroscopy, we observe Ho^{3+} in SEM−EDS measurements of Ho^{3+}−catechol films and posit that minor amounts of the lanthanide metal center may be retained within the network via interactions between catechol hydroxyls and lanthanide metal ions.[76,77] These results are consistent with expectations of improved stability and increased lanthanide capture of HOPO−lanthanide complexes relative to those of the corresponding catechol materials. In addition, the ability to pattern HOPO-functionalized networks allows magnetic heterogeneity to be introduced in addition to the mechanical heterogeneity discussed above. Utilizing the same Ho^{3+}-HOPO patterned sample, we demonstrate the ability to prepare

https://doi.org/10.1021/acs.macromol.4c02250
Macromolecules 2024, 57, 11339−11349

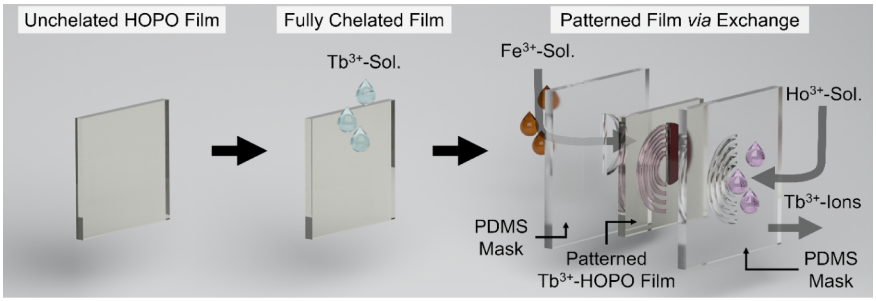

Figure 7. 3D rendering of selective patterning and installation of different metal cations into HOPO-functionalized networks via initial Tb^{3+} complexation followed by a cation exchange using modular patterning approaches. (Left) An untreated HOPO network. (Middle) A fully complexed Tb^{3+}–HOPO network. (Right) Simultaneous top and bottom surface patterning of Fe^{3+} and Ho^{3+} by exchange with Tb^{3+} metal centers.

contiguous polymer networks with heterogeneous magnetic behavior. As observed in Figure 6c and Movie S1, the metal-free control sample and metal-free regions of the patterned sample display negligible magnetic response to a benchtop magnet. Conversely, the holmium Ho^{3+} patterned region of the film displays a strong paramagnetic response and enables the entire patterned sample to be raised. It should be noted that these synthetic approaches are compatible with a wide array of polyacrylate and related network chemistries and may enable development of novel material libraries for soft-robotics applications and magnetic tweezer systems.[15,78−80]

An important feature of the HOPO chemistry is the ability to predictably exchange metal centers, which allows the HOPO unit to bind both transition metals, such as Fe, as well as a range of lanthanides, such as Ho and Tb. This range of lanthanide metal ions offer attractive properties when chelated including paramagnetism and UV induced fluorescence with large, diagnostic Stokes shifts.[18,32,81] By leveraging the ability to exchange lanthanide ions,[82,83] coupled with the strong binding of Fe^{3+} with HOPO,[45] we demonstrate the ability to pattern the negative or "dark" image onto fluorescent Tb^{3+}–HOPO films via exchange and installation of nonfluorescent metal centers. As shown graphically in Figure 7, this allows complex patterned samples to be prepared with localized fluorescence through the chelation and exchange of terbium metal centers.

The complexity of the patterned network structures that can be achieved with this strategy is demonstrated in Figure 8a. In this case, an untreated 3/39/58 mol % PEGDA/PEGMEA/HOPO film is initially fully exposed to Tb^{3+} cations leading to a formation of a secondary Tb^{3+}–HOPO network throughout the original PEGDA covalent network. Masking of this bulk Tb^{3+}–HOPO material is then achieved by placement of patterned PDMS films on both the top surface and the bottom surface of the PEGDA films. The top surface or bottom surface of the Tb^{3+}–HOPO film is then exposed to aqueous solutions of Ho^{3+} and Fe^{3+} ions, respectively. The exposed areas undergo exchange of metal centers resulting in patterned areas of Ho^{3+}–HOPO or Fe^{3+}–HOPO networks within overall Tb^{3+}–HOPO films. As can be seen in Figure 8b, the areas of the original Tb^{3+}–HOPO film appear green under 254 nm light with a negative "dark" pattern being achieved through exchange of the fluorescent Tb^{3+} centers with nonfluorescent holmium and iron metal cations. Significantly, the versatility of this strategy combined with the range of potential transition metal and lanthanide cations allows for potential applications in information storage and encryption[18,84] through selection of different combinations of metal centers.

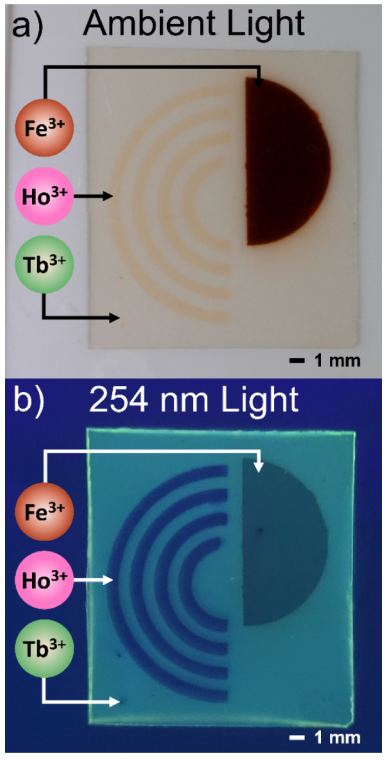

Figure 8. (a) Image of a polymer film of 3/39/58 mol % PEGDA/PEGMEA/HOPO under ambient light after complexation with Tb^{3+} and patterning of Ho^{3+} and Fe^{3+} ions via metal center exchange, with representative metal-ion-containing areas denoted via the guide at left. (b) Image of a polymer film of 3/39/58 mol % PEGDA/PEGMEA/HOPO under UV light (254 nm). Here Tb^{3+}-complexed regions of the film appear green while Ho^{3+} and Fe^{3+} patterned surfaces do not fluorescence.

Detailed characterization of the metal ion patterning was then achieved by scanning electron microscopy–energy dispersive X-ray spectroscopy (SEM–EDS) measurements, which highlight the fidelity and degree of control with this metal ion exchange strategy (Figure 9). For both Ho^{3+} and Fe^{3+} exchange, the significant increase in Ho^{3+} and Fe^{3+} content can be directly correlated with the original exposed areas of the PDMS patterned masks as well as with a corresponding decrease in Tb^{3+} content. It should be noted that SEM–EDS also demonstrated the facile preparation of homogeneous, gradient, and surface patterned materials in the *z*-direction through exchange conditions (Supporting Information). These results highlight the modularity of this strategy for

https://doi.org/10.1021/acs.macromol.4c02250
Macromolecules 2024, 57, 11339−11349

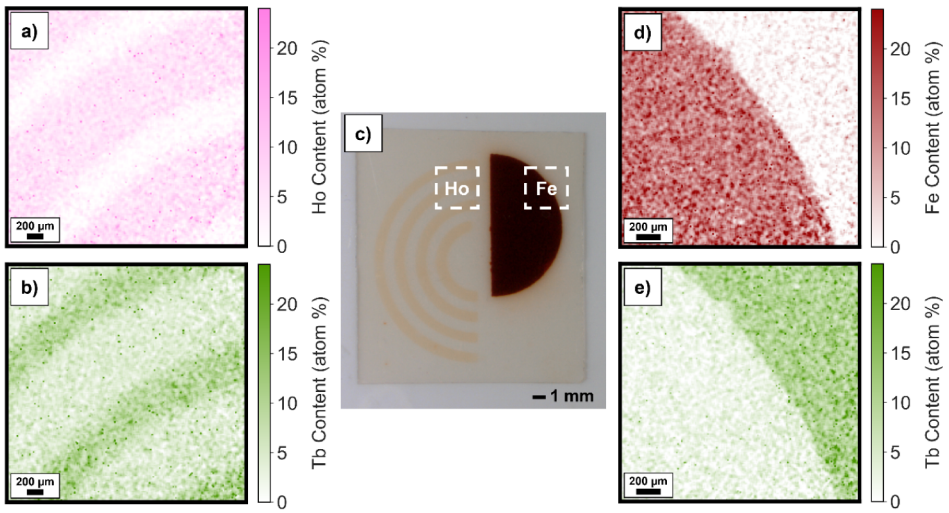

Figure 9. Scanning electron microscopy (SEM)−energy dispersive X-ray spectroscopy (EDS) measurements of metal ion distribution in patterned films. (a) Ho content (atom %) in surface patterned regions and (b) residual Tb content (atom %) after exchange. (c) Image displaying surface patterned film. (d) Fe surface patterned region with respective metal content (atom %), and (e) residual Tb signal (atom %) after displacement in patterned domain.

controlled incorporation of metal ions in tandem with targeted property installation and suggest the utility of this strategy for preparing various surface patterned materials with desirable properties and localized mechanical, magnetic, and fluorescent responses.

CONCLUSION

The versatility of this network strategy based on dual cross-linking modes of covalent PEG-diacrylate cross-links and metal−ligand cross-links using scalable hydroxypyridinone (HOPO) building blocks is demonstrated. When compared to traditional catechol systems, the corresponding HOPO-functionalized materials are shown to display increased oxidative stability and enhanced chelation for lanthanide metal ions. This allows for tailored mechanical, magnetic, and luminescent properties while retaining the advantages of a robust double network. Through facile metal ion exchange, these films can also be patterned with multiple cations while retaining excellent fidelity in the *x*-, *y*-, and *z*-directions. Future work will enable the development of novel multimaterial systems for magnetic tweezers, soft-robotic materials, and selective membranes for lanthanide capture and recovery.

ASSOCIATED CONTENT

Supporting Information

The Supporting Information is available free of charge at https://pubs.acs.org/doi/10.1021/acs.macromol.4c02250.

Experimental methods, sample property tables, and additional data (PDF)

Demonstration of sample magnetic behavior (AVI)

AUTHOR INFORMATION

Corresponding Authors

Matthew E. Helgeson − *Department of Chemical Engineering, University of California, Santa Barbara, Santa Barbara, California 93106-5080, United States;* orcid.org/0000-0001-9384-4023; Email: helgeson@engineering.ucsb.edu

Megan T. Valentine − *Department of Mechanical Engineering, University of California, Santa Barbara, Santa Barbara, California 93106-5070, United States;* orcid.org/0000-0003-4781-8478; Email: valentine@engineering.ucsb.edu

Craig J. Hawker − *Materials Department, University of California Santa Barbara, Santa Barbara, California 93106-5050, United States; Department of Chemistry & Biochemistry, University of California Santa Barbara, Santa Barbara, California 93106-9510, United States; Materials Research Laboratory, University of California Santa Barbara, Santa Barbara, California 93106-5121, United States;* orcid.org/0000-0001-9951-851X; Email: hawker@mrl.ucsb.edu

Authors

Declan P. Shannon − *Materials Department, University of California Santa Barbara, Santa Barbara, California 93106-5050, United States; Materials Research Laboratory, University of California Santa Barbara, Santa Barbara, California 93106-5121, United States*

Kenneth Cerdan − *Department of Mechanical Engineering, University of California, Santa Barbara, Santa Barbara, California 93106-5070, United States; Department of Chemical Engineering, University of California, Santa Barbara, Santa Barbara, California 93106-5080, United States*

Minseong Kim − *Materials Department, University of California Santa Barbara, Santa Barbara, California 93106-5050, United States; Materials Research Laboratory, University of California Santa Barbara, Santa Barbara, California 93106-5121, United States*

Matthew Mecklenburg − *California NanoSystems Institute, University of California, Los Angeles, California 90095, United States;* orcid.org/0000-0003-0581-4153

Judy Su − *California NanoSystems Institute, University of California, Los Angeles, California 90095, United States*

Yueyun Chen − *California NanoSystems Institute, University of California, Los Angeles, California 90095, United States; Department of Physics and Astronomy, University of California, Los Angeles, California 90095, United States;* orcid.org/0009-0008-4325-068X

Complete contact information is available at:

https://pubs.acs.org/10.1021/acs.macromol.4c02250

Notes

The authors declare no competing financial interest.

■ ACKNOWLEDGMENTS

The support for this research is provided by the National Science Foundation, Division of Materials Research under the BioPACIFIC Materials Innovation Platform (Award No. DMR 1933487). K.C. and M.E.H. received partial support from the MRSEC Program of the National Science Foundation under Award No. DMR 2308708 (IRG-2). K.C. was partially supported by the NSF under Award No. DMR-2004937 (to M.T.V.). The authors also acknowledge the use of the MRL Shared Experimental Facilities, supported by the MRSEC Program of the NSF under Award No. DMR 2308708; a member of the NSF-funded Materials Research Facilities Network (www.mrfn.org), the Microfluidics Laboratory and Quantum Structures Facility within the California NanoSystems Institute (CNSI) supported by the University of California, Santa Barbara, Office of the President. The authors acknowledge additional support from the optical characterization facility housed in the University of California, Santa Barbara, Department of Chemistry and Biochemistry. Scanning electron microscopy data was acquired with instruments at the Electron Imaging Center for NanoSystems (EICN) at the University of California, Los Angeles's California for NanoSystems Institute (CNSI) (RRID:SCR_022900).

■ REFERENCES

(1) Zhao, X.; Chen, X.; Yuk, H.; Lin, S.; Liu, X.; Parada, G. Soft Materials by Design: Unconventional Polymer Networks Give Extreme Properties. *Chem. Rev.* **2021**, *121* (8), 4309−4372.

(2) Ganewatta, M. S.; Wang, Z.; Tang, C. Chemical Syntheses of Bioinspired and Biomimetic Polymers toward Biobased Materials. *Nat. Rev. Chem.* **2021**, *5* (11), 753−772.

(3) Khare, E.; Holten-Andersen, N.; Buehler, M. J. Transition-Metal Coordinate Bonds for Bioinspired Macromolecules with Tunable Mechanical Properties. *Nat. Rev. Mater.* **2021**, *6* (5), 421−436.

(4) Bailey, S. J.; Hopkins, E.; Baxter, N. J.; Whitehead, I.; de Alaniz, J. R.; Wilson, M. Z. Diels−Alder Photoclick Patterning of Extracellular Matrix for Spatially Controlled Cell Behaviors. *Adv. Mater.* **2023**, *35* (46), 2303453.

(5) Lin, X.; Wang, X.; Zeng, L.; Wu, Z. L.; Guo, H.; Hourdet, D. Stimuli-Responsive Toughening of Hydrogels. *Chem. Mater.* **2021**, *33* (19), 7633−7656.

(6) Garcia, R. V.; Murphy, E. A.; Sinha, N. J.; Okayama, Y.; Urueña, J. M.; Helgeson, M. E.; Bates, C. M.; Hawker, C. J.; Murphy, R. D.; Read de Alaniz, J. Tailoring Writability and Performance of Star Block Copolypeptides Hydrogels through Side-Chain Design. *Small* **2023**, *19* (50), 2302794.

(7) Ducrot, E.; Chen, Y.; Bulters, M.; Sijbesma, R. P.; Creton, C. Toughening Elastomers with Sacrificial Bonds and Watching Them Break. *Science* **2014**, *344* (6180), 186−189.

(8) Liu, J.; Tan, C. S. Y.; Yu, Z.; Li, N.; Abell, C.; Scherman, O. A. Tough Supramolecular Polymer Networks with Extreme Stretchability and Fast Room-Temperature Self-Healing. *Adv. Mater.* **2017**, *29* (22), 1605325.

(9) Vashahi, F.; Martinez, M. R.; Dashtimoghadam, E.; Fahimipour, F.; Keith, A. N.; Bersenev, E. A.; Ivanov, D. A.; Zhulina, E. B.; Popryadukhin, P.; Matyjaszewski, K.; Vatankhah-Varnosfaderani, M.; Sheiko, S. S. Injectable Bottlebrush Hydrogels with Tissue-Mimetic Mechanical Properties. *Sci. Adv.* **2022**, *8* (3), No. eabm2469.

(10) Holten-Andersen, N.; Harrington, M. J.; Birkedal, H.; Lee, B. P.; Messersmith, P. B.; Lee, K. Y. C.; Waite, J. H. pH-Induced Metal-Ligand Cross-Links Inspired by Mussel Yield Self-Healing Polymer Networks with near-Covalent Elastic Moduli. *Proc. Natl. Acad. Sci. U. S. A.* **2011**, *108* (7), 2651−2655.

(11) Capadona, J. R.; Shanmuganathan, K.; Tyler, D. J.; Rowan, S. J.; Weder, C. Stimuli-Responsive Polymer Nanocomposites Inspired by the Sea Cucumber Dermis. *Science* **2008**, *319* (5868), 1370−1374.

(12) Kim, S.; Regitsky, A. U.; Song, J.; Ilavsky, J.; McKinley, G. H.; Holten-Andersen, N. In Situ Mechanical Reinforcement of Polymer Hydrogels via Metal-Coordinated Crosslink Mineralization. *Nat. Commun.* **2021**, *12* (1), 667.

(13) Timonen, J. V. I.; Grzybowski, B. A. Tweezing of Magnetic and Non-Magnetic Objects with Magnetic Fields. *Adv. Mater.* **2017**, *29* (18), 1603516.

(14) Strick, T. R.; Allemand, J.-F.; Bensimon, D.; Bensimon, A.; Croquette, V. The Elasticity of a Single Supercoiled DNA Molecule. *Science* **1996**, *271* (5257), 1835−1837.

(15) Kim, Y.; Zhao, X. Magnetic Soft Materials and Robots. *Chem. Rev.*. **2022**, *122* (5), 5317−5364.

(16) Li, Z.; Li, Y.; Chen, C.; Cheng, Y. Magnetic-Responsive Hydrogels: From Strategic Design to Biomedical Applications. *J. Controlled Release* **2021**, *335*, 541−556.

(17) Li, C.; Lau, G. C.; Yuan, H.; Aggarwal, A.; Dominguez, V. L.; Liu, S.; Sai, H.; Palmer, L. C.; Sather, N. A.; Pearson, T. J.; Freedman, D. E.; Amiri, P. K.; de la Cruz, M. O.; Stupp, S. I. Fast and Programmable Locomotion of Hydrogel-Metal Hybrids under Light and Magnetic Fields. *Sci. Rob.* **2020**, *5* (49), No. eabb9822.

(18) Feng, Y.; White, A. K.; Hein, J. B.; Appel, E. A.; Fordyce, P. M. MRBLES 2.0: High-Throughput Generation of Chemically Functionalized Spectrally and Magnetically Encoded Hydrogel Beads Using a Simple Single-Layer Microfluidic Device. *Microsyst. Nanoeng.* **2020**, *6* (1), 1−13.

(19) Yin, Q.; Wang, L.; Jiang, J.; Dai, C.; Weng, G.; He, J. Three-Dimensional Shape Transformation of Eu3+-Containing Polymer Films through Modulating Dynamic Eu3+-Iminodiacetate Coordination. *Chem. Mater.* **2022**, *34* (5), 2176−2186.

(20) Filippidi, E.; Cristiani, T. R.; Eisenbach, C. D.; Waite, J. H.; Israelachvili, J. N.; Ahn, B. K.; Valentine, M. T. Toughening Elastomers Using Mussel-Inspired Iron-Catechol Complexes. *Science* **2017**, *358* (6362), 502−505.

(21) Shannon, D. P.; Moon, J. D.; Barney, C. W.; Sinha, N. J.; Yang, K.-C.; Jones, S. D.; Garcia, R. V.; Helgeson, M. E.; Segalman, R. A.; Valentine, M. T.; Hawker, C. J. Modular Synthesis and Patterning of High-Stiffness Networks by Postpolymerization Functionalization with Iron−Catechol Complexes. *Macromolecules* **2023**, *56* (6), 2268−2276.

(22) Weng, G.; Thanneeru, S.; He, J. Dynamic Coordination of Eu−Iminodiacetate to Control Fluorochromic Response of Polymer Hydrogels to Multistimuli. *Adv. Mater.* **2018**, *30* (11), 1706526.

(23) Beck, J. B.; Rowan, S. J. Multistimuli, Multiresponsive Metallo-Supramolecular Polymers. *J. Am. Chem. Soc.* **2003**, *125* (46), 13922−13923.

(24) Winter, A.; Schubert, U. S. Synthesis and Characterization of Metallo-Supramolecular Polymers. *Chem. Soc. Rev.* **2016**, *45* (19), 5311−5357.

(25) Mozhdehi, D.; Neal, J. A.; Grindy, S. C.; Cordeau, Y.; Ayala, S.; Holten-Andersen, N.; Guan, Z. Tuning Dynamic Mechanical Response in Metallopolymer Networks through Simultaneous Control of Structural and Temporal Properties of the Networks. *Macromolecules* **2016**, *49* (17), 6310−6321.

(26) Grindy, S. C.; Learsch, R.; Mozhdehi, D.; Cheng, J.; Barrett, D. G.; Guan, Z.; Messersmith, P. B.; Holten-Andersen, N. Control of Hierarchical Polymer Mechanics with Bioinspired Metal-Coordination Dynamics. *Nat. Mater.* **2015**, *14* (12), 1210−1216.

(27) Du, L.; Xu, Z.-Y.; Fan, C.-J.; Xiang, G.; Yang, K.-K.; Wang, Y.-Z. A Fascinating Metallo-Supramolecular Polymer Network with Thermal/Magnetic/Light-Responsive Shape-Memory Effects Anchored by Fe3O4 Nanoparticles. *Macromolecules* **2018**, *51* (3), 705−715.

(28) Shi, L.; Ding, P.; Wang, Y.; Zhang, Y.; Ossipov, D.; Hilborn, J. Self-Healing Polymeric Hydrogel Formed by Metal−Ligand Coordi-

nation Assembly: Design, Fabrication, and Biomedical Applications. *Macromol. Rapid Commun.* **2019**, *40* (7), 1800837.
(29) Moon, J. D.; Sujanani, R.; Geng, Z.; Freeman, B. D.; Segalman, R. A.; Hawker, C. J. Versatile Synthetic Platform for Polymer Membrane Libraries Using Functional Networks. *Macromolecules* **2021**, *54* (2), 866−873.
(30) Johnson, L.; Schneider, B. L.; Mithaiwala, H.; Green, M. D.; Renner, J. N.; Duval, C. E. Electrospun Membranes Modified with Lanmodulin-Derived Peptides for Lanthanide Adsorption. *ACS Appl. Eng. Mater.* **2024**, *2* (10), 2442−2453.
(31) Suresh, P.; Johnson, L.; Duval, C. E. Membrane Adsorbers with Copolymer Coatings for the Separation of Actinides from Lanthanides (UO22+ and La3+). *Ind. Eng. Chem. Res.* **2024**, *63*, 20373.
(32) Yamamoto, M.; Ando, K.; Inoue, M.; Kanoh, H.; Yamagami, M.; Wakiya, T.; Iida, E.; Taniguchi, T.; Kishikawa, K.; Kohri, M. Poly-*β*-Ketoester Particles as a Versatile Scaffold for Lanthanide-Doped Colorless Magnetic Materials. *ACS Appl. Polym. Mater.* **2020**, *2* (6), 2170−2178.
(33) Harrington, M. J.; Masic, A.; Holten-Andersen, N.; Waite, J. H.; Fratzl, P. Iron-Clad Fibers: A Metal-Based Biological Strategy for Hard Flexible Coatings. *Science* **2010**, *328* (5975), 216−220.
(34) Joester, D.; Brooker, L. R. The Chiton Radula: A Model System for Versatile Use of Iron Oxides. In *Iron Oxides: From nature to applications*; John Wiley & Sons, Ltd, 2016, pp. 177−206. DOI: .
(35) Lichtenegger, H. C.; Schöberl, T.; Ruokolainen, J. T.; Cross, J. O.; Heald, S. M.; Birkedal, H.; Waite, J. H.; Stucky, G. D. Zinc and Mechanical Prowess in the Jaws of Nereis, a Marine Worm. *Proc. Natl. Acad. Sci. U. S. A.* **2003**, *100* (16), 9144−9149.
(36) Politi, Y.; Priewasser, M.; Pippel, E.; Zaslansky, P.; Hartmann, J.; Siegel, S.; Li, C.; Barth, F. G.; Fratzl, P. A Spider's Fang: How to Design an Injection Needle Using Chitin-Based Composite Material. *Adv. Funct. Mater.* **2012**, *22* (12), 2519−2528.
(37) Wonderly, W. R.; Nguyen, T. T. D.; Malollari, K. G.; DeMartini, D.; Delparastan, P.; Valois, E.; Messersmith, P. B.; Helgeson, M. E.; Waite, J. H. A Multi-Tasking Polypeptide from Bloodworm Jaws: Catalyst, Template, and Copolymer in Film Formation. *Matter* **2022**, *5* (6), 1890−1908.
(38) Lee, S.; Kustin, K.; Robinson, W. E.; Frankel, R. B.; Spartalian, K. Magnetic Properties of Tunicate Blood Cells. I. Ascidia Nigra. *J. Inorg. Biochem.* **1988**, *33* (3), 183−192.
(39) Fung, T.-M.; Gallego Lazo, C.; Smith, A. M. Elasticity and Energy Dissipation in the Double Network Hydrogel Adhesive of the Slug Arion Subfuscus. *Philos. Trans. R. Soc., B* **2019**, *374* (1784), 20190201.
(40) Raymond, K. N.; Allred, B. E.; Sia, A. K. Coordination Chemistry of Microbial Iron Transport. *Acc. Chem. Res.* **2015**, *48* (9), 2496−2505.
(41) Sandy, M.; Butler, A. Microbial Iron Acquisition: Marine and Terrestrial Siderophores. *Chem. Rev.* **2009**, *109* (10), 4580−4595.
(42) Cook, E. C.; Featherston, E. R.; Showalter, S. A.; Cotruvo, J. A. Jr Structural Basis for Rare Earth Element Recognition by Methylobacterium Extorquens Lanmodulin. *Biochemistry* **2019**, *58* (2), 120−125.
(43) Cotruvo, J. A. J.; Featherston, E. R.; Mattocks, J. A.; Ho, J. V.; Laremore, T. N. Lanmodulin: A Highly Selective Lanthanide-Binding Protein from a Lanthanide-Utilizing Bacterium. *J. Am. Chem. Soc.* **2018**, *140* (44), 15056−15061.
(44) Cotruvo, J. A., Jr The Chemistry of Lanthanides in Biology: Recent Discoveries, Emerging Principles, and Technological Applications. *ACS Cent. Sci.* **2019**, *5* (9), 1496−1506.
(45) Cilibrizzi, A.; Abbate, V.; Chen, Y.-L.; Ma, Y.; Zhou, T.; Hider, R. C. Hydroxypyridinone Journey into Metal Chelation. *Chem. Rev.* **2018**, *118* (16), 7657−7701.
(46) Raymond, K. N. Biomimetic Metal Encapsulation. *Coord. Chem. Rev.* **1990**, *105*, 135−153.
(47) Tanaka, K.; Tengeiji, A.; Kato, T.; Toyama, N.; Shiro, M.; Shionoya, M. Efficient Incorporation of a Copper Hydroxypyridone Base Pair in DNA. *J. Am. Chem. Soc.* **2002**, *124* (42), 12494−12498.
(48) Datta, A.; Raymond, K. N. Gd−Hydroxypyridinone (HOPO)-Based High-Relaxivity Magnetic Resonance Imaging (MRI) Contrast Agents. *Acc. Chem. Res.* **2009**, *42* (7), 938−947.
(49) Honda, M. D. H.; Borthakur, D. Mimosine Facilitates Metallic Cation Uptake by Plants through Formation of Mimosine−Cation Complexes. *Plant Mol. Biol.* **2020**, *102* (4), 431−445.
(50) Honda, M. D. H.; Borthakur, D. Mimosine Facilitates Fe Uptake by Leucaena Leucocephala Subsp. Glabrata in Alkaline Soils by Solubilizing Fe-Oxides. *Plant Soil* **2023**, *484* (1), 279−292.
(51) Andersen, A.; Krogsgaard, M.; Birkedal, H. Mussel-Inspired Self-Healing Double-Cross-Linked Hydrogels by Controlled Combination of Metal Coordination and Covalent Cross-Linking. *Biomacromolecules* **2018**, *19* (5), 1402−1409.
(52) Mendonça, A. C.; Martins, A. F.; Melchior, A.; Marques, S. M.; Chaves, S.; Villette, S.; Petoud, S.; Zanonato, P. L.; Tolazzi, M.; Bonnet, C. S.; et al. New Tris-3,4-HOPO Lanthanide Complexes as Potential Imaging Probes: Complex Stability and Magnetic Properties. *Dalton Trans.* **2013**, *42* (17), 6046−6057.
(53) Wang, Y.; Deblonde, G. J.-P.; Abergel, R. J. Hydroxypyridinone Derivatives: A Low-pH Alternative to Polyaminocarboxylates for TALSPEAK-like Separation of Trivalent Actinides from Lanthanides. *ACS Omega* **2020**, *5* (22), 12996−13005.
(54) Puerta, D. T.; Lewis, J. A.; Cohen, S. M. New Beginnings for Matrix Metalloproteinase Inhibitors: Identification of High-Affinity Zinc-Binding Groups. *J. Am. Chem. Soc.* **2004**, *126* (27), 8388−8389.
(55) Menyo, M. S.; Hawker, C. J.; Waite, J. H. Versatile Tuning of Supramolecular Hydrogels through Metal Complexation of Oxidation-Resistant Catechol-Inspired Ligands. *Soft Matter* **2013**, *9* (43), 10314−10323.
(56) Chaves, S.; Gwizdała, K.; Chand, K.; Gano, L.; Pallier, A.; Tóth, É.; Santos, M. A. Gd III and Ga III Complexes with a New Tris-3,4-HOPO Ligand as New Imaging Probes: Complex Stability, Magnetic Properties and Biodistribution. *Dalton Trans.* **2022**, *51* (16), 6436−6447.
(57) Cen, J.; Zhu, H.; Hong, C.; Zhang, X.; Liu, S.; Yang, B.; Yu, Y.; Wen, Y.; Cao, J.; Chen, W. Synthesis and Structure-Activity Optimization of Hydroxypyridinones against Rhabdomyolysis-Induced Acute Kidney Injury. *Eur. J. Med. Chem.* **2024**, *263*, 115933.
(58) Santos, M. A.; Marques, S. M.; Chaves, S. Hydroxypyridinones as "Privileged" Chelating Structures for the Design of Medicinal Drugs. *Coord. Chem. Rev.* **2012**, *256* (1), 240−259.
(59) Menyo, M. S.; Hawker, C. J.; Waite, J. H. Rate-Dependent Stiffness and Recovery in Interpenetrating Network Hydrogels through Sacrificial Metal Coordination Bonds. *ACS Macro Lett.* **2015**, *4* (11), 1200−1204.
(60) Ke, D.; Zhang, L.; Zhong, X.; Shao, J.; Yu, Y.; Chen, W. Boronic-Acid-Accelerated Electrophilic Activation of Unprotected Maltols to N-Substituted Hydroxypyridinones in Water. *Org. Lett.* **2022**, *24* (6), 1263−1267.
(61) Kohaku, K.; Inoue, M.; Kanoh, H.; Taniguchi, T.; Kishikawa, K.; Kohri, M. Full-Color Magnetic Nanoparticles Based on Holmium-Doped Polymers. *ACS Appl. Polym. Mater.* **2020**, *2* (5), 1800−1806.
(62) Jiang, F.; Wang, Z.; Zhang, X.; Henderson, D.; Hwang, W.; Briber, R. M.; Wang, H. Synergistically Tailoring Mechanical and Optical Properties of Diblock Copolymer Thermoplastic Elastomers via Lanthanide Coordination. *Chem. Mater.* **2022**, *34* (4), 1578−1589.
(63) Gomes, M. C.; Costa, D. C. S.; Oliveira, C. S.; Mano, J. F. Design of Protein-Based Liquefied Cell-Laden Capsules with Bioinspired Adhesion for Tissue Engineering. *Adv. Healthcare Mater.* **2021**, *10* (19), 2100782.
(64) De Molina, P. M.; Lad, S.; Helgeson, M. E. Heterogeneity and Its Influence on the Properties of Difunctional Poly(Ethylene Glycol) Hydrogels: Structure and Mechanics. *Macromolecules* **2015**, *48* (15), 5402−5411.
(65) Cristiani, T. R.; Filippidi, E.; Behrens, R. L.; Valentine, M. T.; Eisenbach, C. D. Tailoring the Toughness of Elastomers by Incorporating Ionic Cross-Linking. *Macromolecules* **2020**, *53* (10), 4099−4109.

https://doi.org/10.1021/acs.macromol.4c02250
Macromolecules 2024, 57, 11339−11349

(66) Beija, M.; Li, Y.; Lowe, A. B.; Davis, T. P.; Boyer, C. Factors Influencing the Synthesis and the Post-Modification of PEGylated Pentafluorophenyl Acrylate Containing Copolymers. *Eur. Polym. J.* **2013**, *49* (10), 3060−3071.
(67) Barrett, D. G.; Fullenkamp, D. E.; He, L.; Holten-Andersen, N.; Lee, K. Y. C.; Messersmith, P. B. pH-Based Regulation of Hydrogel Mechanical Properties Through Mussel-Inspired Chemistry and Processing. *Adv. Funct. Mater.* **2013**, *23* (9), 1111−1119.
(68) Yang, J.; Cohen Stuart, M. A.; Kamperman, M. Jack of All Trades: Versatile Catechol Crosslinking Mechanisms. *Chem. Soc. Rev.* **2014**, *43* (24), 8271−8298.
(69) Pillar-Little, E. A.; Zhou, R.; Guzman, M. I. Heterogeneous Oxidation of Catechol. *J. Phys. Chem. A* **2015**, *119* (41), 10349−10359.
(70) Lagutschenkov, A.; Langer, J.; Berden, G.; Oomens, J.; Dopfer, O. Infrared Spectra of Protonated Neurotransmitters: Dopamine. *Phys. Chem. Chem. Phys.* **2011**, *13* (7), 2815−2823.
(71) Zangmeister, R. A.; Morris, T. A.; Tarlov, M. J. Characterization of Polydopamine Thin Films Deposited at Short Times by Autoxidation of Dopamine. *Langmuir* **2013**, *29* (27), 8619−8628.
(72) Šebestík, J.; Šafařík, M.; Bouř, P. Ferric Complexes of 3-Hydroxy-4-Pyridinones Characterized by Density Functional Theory and Raman and UV−Vis Spectroscopies. *Inorg. Chem.* **2012**, *51* (8), 4473−4481.
(73) Jianlin, Y.; Yaxian, Y.; Renao, G. Raman Spectroscopic Studies on Tropolone Complexes with La, Nd, Sm, Yb. *Spectrochim. Acta, Part A* **2006**, *64* (4), 1072−1076.
(74) Burden, K. J.; Thornton, D. A.; Watkins, G. M. A Re-Examination of the Infrared Spectra of First Transition Series Metal(II) and Metal(III) Tropolonates. *Spectrochim. Acta, Part A* **1989**, *45* (11), 1179−1186.
(75) Parajón-Costa, B. S.; Baran, E. J.; Romero, J.; Sáez-Puche, R.; Arrambide, G.; Gambino, D. Synthesis and Characterization of Bistropolonato Oxovanadium(IV and V) Complexes. *J. Coord. Chem.* **2011**, *64* (1), 57−70.
(76) Zhu, D.-H.; Kappel, M. J.; Raymond, K. N. Coordination Chemistry of Lanthanide Catecholates. *Inorg. Chim. Acta* **1988**, *147* (1), 115−121.
(77) Menyo, M. S. *Fine-Tuning Catechol Reactivity in Synthetic Polymeric Materials*; UC Santa Barbara, 2015. https://escholarship.org/uc/item/81n7232w (accessed 2024−September−17).
(78) Xin, Q.; Li, P.; He, Y.; Shi, C.; Qiao, Y.; Bian, X.; Su, J.; Qiao, R.; Zhou, X.; Zhong, J. Magnetic Tweezers for the Mechanical Research of DNA at the Single Molecule Level. *Anal. Methods* **2017**, *9* (39), 5720−5730.
(79) Pena-Francesch, A.; Zhang, Z.; Marks, L.; Cabanach, P.; Richardson, K.; Sheehan, D.; McCracken, J.; Shahsavan, H.; Sitti, M. Macromolecular Radical Networks for Organic Soft Magnets. *Matter* **2024**, *7* (4), 1503−1516.
(80) Ebrahimi, N.; Bi, C.; Cappelleri, D. J.; Ciuti, G.; Conn, A. T.; Faivre, D.; Habibi, N.; Hošovský, A.; Iacovacci, V.; Khalil, I. S. M.; Magdanz, V.; Misra, S.; Pawashe, C.; Rashidifar, R.; Soto-Rodriguez, P. E. D.; Fekete, Z.; Jafari, A. Magnetic Actuation Methods in Bio/Soft Robotics. *Adv. Funct. Mater.* **2021**, *31* (11), 2005137.
(81) Bünzli, J.-C. G. Lanthanide Luminescence for Biomedical Analyses and Imaging. *Chem. Rev.* **2010**, *110* (5), 2729−2755.
(82) Cheisson, T.; Schelter, E. J. Rare Earth Elements: Mendeleev's Bane, Modern Marvels. *Science* **2019**, *363* (6426), 489−493.
(83) Martell, A. E.; Smith, R. M. *Critical Stability Constants: First Supplement*; Springer US: Boston, MA, 1982. DOI: .
(84) Zhou, Y.; Hao, K.; Liu, C.; Yu, R.; Huang, A.; Wu, C.; Yang, Y.; Zuo, X. 3D Printed Hydrogels with Time/Temperature-Dependent Photoluminescence for Multi-Information Dynamic Display. *ACS Appl. Polym. Mater.* **2024**, *6* (3), 2012−2021.

https://doi.org/10.1021/acs.macromol.4c02250
Macromolecules 2024, 57, 11339−11349